

R. BIDULSKÝ<sup>①,2\*</sup>, P. PETROUŠEK<sup>③</sup>, J. BIDULSKÁ<sup>③</sup>, R. HUDÁK<sup>④</sup>,  
J. ŽIVČÁK<sup>④</sup>, M. ACTIS GRANDE<sup>①</sup>

## POROSITY QUANTIFICATION OF ADDITIVE MANUFACTURED Ti6Al4V AND CoCrW ALLOYS PRODUCED BY L-PBF

The main aim of the present paper is to evaluate the porosity and mechanical properties of Ti6Al4V and CoCrW alloys produced by Laser Powder Bed Fusion (L-PBF) as an additive manufacturing (AM) technology. Ti6Al4V and CoCrW alloys are attractive for medical application. The complex examination of porosity for these alloys needs the quantification of morphological and dimensional characteristics. Quantification of porosity was realized on non-etched samples. Quantitative image analysis was used to describe the dimensional and morphological porosity characteristics. The pores were evaluated by Image pro plus software. The results show the significant inhomogeneity of the morphology and distribution, as well as the pore size in the investigated materials and underline the importance of pore structure for the controlling mechanism of the mechanical response.

**Keywords:** Powder metallurgy; additive manufacturing; porosity; Ti6Al4V; CoCrW

### 1. Introduction

The concept of powder bed fusion (PBF) includes a wide range of technologies based on the principle of additive manufacturing (AM) of powdered metallic materials. The key to this technology is the correct setting of the instrument to achieve the best mechanical properties. The resulting mechanical properties depend on many parameters of AM built process. There is a large number of research papers focused on the influence of different parameters on the microstructure and final mechanical properties of products [1-6], but the porosity structure as a critical factor for assessing of desired mechanical properties is still welcome for a better understanding of the processing phenomena of AM.

Porosity is a common defect in AM products since most of the binding mechanisms are driven by temperature changes, gravity and capillary forces without applying external pressure. Porosity can be found as irregular pores (e.g., due to shrinkage, lack of binding/fusion/melting, or material feed shortage, often occurring at the border of molten tracks) or spherical pores (commonly due to trapped gas, Marangoni turbulences in the melt region, material evaporation, etc., often occurring within the molten tracks) [7-9].

In all, the density of laser powder bed fusion (L-PBF) produced parts are highly dependent on scanning speed, through which controlling the porosity is possible. It is known that the mechanical performance of a part is an essential parameter for assessment of its final practicability [10]. The titanium alloy system Ti6Al4V and CoCr-based alloys are very popular AM materials due to their implementation in medical applications [11].

Ti6Al4V components prepared by the L-PBF technology can overdraw the tensile properties of conventionally manufactured materials [12]. On the other side, the poor fatigue and wear resistance in additively manufactured titanium alloys is caused by high porosity levels. There have been multiple types of porosity observed in these materials [12-18].

The presence of fusion porosity is created by the insufficient melting of a new layer of powder to an early deposited layer, or between contiguous beam passes. These pores are >100 µm in size and have an irregular shape [19].

This paper covers Ti6Al4V and CoCrW alloys since both alloys are attractive for medical applications. The main aim of the proposed research is compared both alloys with respect to the mechanical properties and porosity evaluation. The quality of the proposed alloys is interesting due to the final application

<sup>1</sup> POLITECNICO DI TORINO, DEPARTMENT OF APPLIED SCIENCE AND TECHNOLOGY, CORSO DUCA DEGLI ABRUZZI, 24, 10129 TORINO, ITALY

<sup>2</sup> ASIAN INNOVATION HUB, BUDULOV 174, 045 01 MOLDAVA NAD BODVOU, SLOVAKIA

<sup>3</sup> TECHNICAL UNIVERSITY OF KOSICE, FACULTY OF MATERIALS, METALLURGY AND RECYCLING, DPT. OF PLASTIC DEFORMATION AND PROCESS SIMULATION, LETNÁ 9, 042 00 KOSICE, SLOVAKIA

<sup>4</sup> TECHNICAL UNIVERSITY OF KOSICE, FACULTY OF MECHANICAL ENGINEERING, DPT. OF INSTRUMENTAL AND BIOMEDICAL ENGINEERING, LETNÁ 9, 042 00 KOSICE, SLOVAKIA

\* Corresponding author: robert.bidulsky@polito.it; robert.bidulsky@asihub.org



in the dental crowns [20]. The complex examination of porosity for these alloys also needs the quantification of morphological and dimensional characteristics. The present paper is focused on the structure-function of porosity phenomena by using quantitative image analyses.

## 2. Materials and methods

As experimental materials, the Ti6Al4V (Grade5, Electro Optical Systems, Finland) and CoCrW (Remanium®starCL powered by Dentaurum) powders were used. The samples were prepared by the Mlab Curing R (Concept Laser, Germany), which works by L-PBF technology. The workspace for sample preparation is 90×90×80 mm (x, y, z). The device is equipped with a 100 Watt laser. The dimensions of the samples according to the MPIF Standard Test Methods Edition 2007 are shown in [5,6]. All samples were produced in one batch.

The evaluation of porosity was realized on non-etched samples using optical microscope Zeiss Axiovert A1 equipped with an image analyzer. Characterizations were carried out at 100x magnification on the minimum seven different image fields for specimens prepared by AM technology. The pores were evaluated by Image pro plus software. Quantitative image analysis treats pores as isolated objects in the two-dimensional plane in order to describe the dimensional and morphological porosity characteristics. Morphological characteristics are  $f_{circle}$ ,  $f_{shape}$  (showing the shape of the pores which has a major impact on the mechanical properties):

$$f_{shape} = \frac{D_{min}}{D_{max}} = \frac{a}{b} \quad /-$$
 (1)

where

$D_{min}$  – parameter representing a minimum of Feret diameter, [cm];

$D_{max}$  – parameter representing a maximum of Feret diameter, [cm];

and

$$f_{circle} = \frac{4 \cdot \pi \cdot A}{P^2} \quad /-$$
 (2)

where  $A$  – area of the metallographic cross-section of the pore, [ $\text{cm}^2$ ],

$$A = \pi \cdot a \cdot b \quad (3)$$

where  $P$  – perimeter of the metallographic cross-section of the pore, [cm],

$$P = \pi \left[ 1.5 \cdot (a \cdot b) - \sqrt{a \cdot b} \right] \quad (4)$$

The dimensional characteristic  $D_{circle}$  (representing the diameter of the equivalent circle showing the same area as the metallographic cross-section of the pore) and aspect ratio  $A$  (representing the ratio between the major axis and minor axis of an ellipse equivalent to pore) according to [21-23]. The aspect ratio considers the stress and the strain situation in the process of AM. The evaluation procedure described in more detail is at work [5,6]. From our previous studies [15-17], it's known that nanopores do not affect the mechanism of fracture formation. Therefore, only pores of a size greater than 1  $\mu\text{m}$  were investigated.

Total porosity was calculated by equation [6,19,21,22]:

$$P = \left( 1 - \frac{\rho_g}{\rho_t} \right) \cdot 100 \quad [\%] \quad (5)$$

where

$P$  – total porosity,

$\rho_g$  – green density [ $\text{kg} \cdot \text{m}^{-3}$ ]

$\rho_t$  – theoretical density [ $\text{kg} \cdot \text{m}^{-3}$ ].

Sampled dimensions for sinter-and-press specimens respected the MPIF standard 10 and for ECAPed specimen's dimensions were 10 mm in diameter and 55 mm in length. Samples were tested in a universal servo-hydraulic testing machine Tinius Olsen with a crosshead speed of 0.5  $\text{mm} \cdot \text{min}^{-1}$ . Five measurements were taken from each sample and the average value of three measurements, excluding the highest and lowest values, were recorded.

## 3. Results and discussion

The values of mechanical properties and morphological porosity characteristics are shown in Table 1.

As shown in Table 1, results related to the mechanical properties are in good accordance with other tensile properties achieved for Ti6Al4V alloy by authors [25-27], as well as for CoCrW alloy [28-30]. In spite of the higher level of porosity in Ti6Al4V alloy (4 %), better mechanical properties were obtained: YS was 692 MPa, and TS was 1080 MPa in comparison with CoCrW alloy.

Parts destined for high-stress applications should be fully dense, to minimize the possibility of part failure during service. Degrees of porosity is sometimes desirable and with respect to the fact that both investigated alloys are mostly dedicated to the dental application [20], it can be intentionally engineered into certain bio-medical implants since the pores promote better osseointegration with biological tissue [24].

TABLE 1

Mechanical properties and morphological porosity characteristics of Ti6Al4V and CoCrW alloys

	YS [MPa]	UTS [MPa]	$f_{shape}$ [-]	$f_{circle}$ [-]	$D_{circle}$ [ $\mu\text{m}$ ]	Aspect [-]	Porosity [%]
Ti6Al4V	$692 \pm 73$	$1080 \pm 5$	$0,75 \pm 0,15$	$0,9 \pm 0,1$	$13,2 \pm 32,4$	$1,3 \pm 1,4$	4,4
CoCrW	$559 \pm 30$	$979 \pm 119$	$0,48 \pm 0,2$	$0,63 \pm 0,24$	$22,1 \pm 25,2$	$2,1 \pm 1,7$	2,9

The quantitative image analysis show different porosity behaviour in both investigated alloys. The non-etched microstructures of both alloys are presented in Fig. 1 and Fig. 3. The Fig. 2 and Fig. 4 show both microstructures after evaluation by Image pro plus software. Observing Fig. 4, it is clearly possible to recognize some voids were out from measurement. This Si-rich inclusion leave large residual void behind [11]. This is not pores, principally thanks to the fabrication process, in particular, especially for alloys containing tungsten. The fabrication process is thus affected by the aforementioned factors to form defects [31].

The distribution histograms and the cumulative curves of the porosity behaviour for the Ti6Al4V and CoCrW alloys are presented in Fig. 5 and Fig. 6.

In order to allow a statistical interpretation, the data can be presented in Figs. 5-6 as distribution histograms. Reading the figures can reveal the shape of the distribution. Dimensional characteristics  $D_{circle}$  and Aspect show that values 13  $\mu\text{m}$  for Ti6Al4V and 22  $\mu\text{m}$  for CoCrW are corresponding with

a higher frequency of data. Also, cumulative frequency shows that obtained results of  $D_{circle}$  and Aspect for both investigated alloys represent a value which fully covers the dimensional characteristics of pores.

From the data in Fig. 5, Ti6Al4V, for the yield data of the morphological characteristics, it is noticed that there are for both parameters  $f_{shape}$  and  $f_{circle}$  prevailed bins with 0,8 and 0,9 values. Also, Vilaro et al. [32] observed that the pore shape and orientation strongly influence mechanical properties. On the other hand, it seems that the distribution of CoCrW data appears approximately bell-shaped.

In order to achieve the control of pore structure by tailoring the AM machine parameters, a full understanding of the pore distribution processes is needed. The precise control the manufacturing conditions locally within the part of AM build, enabling local influence on the formation of the pores. Fig. 7 offers a better overview of the presented results. Review paper [27] underlines that a very limited amount of work covered

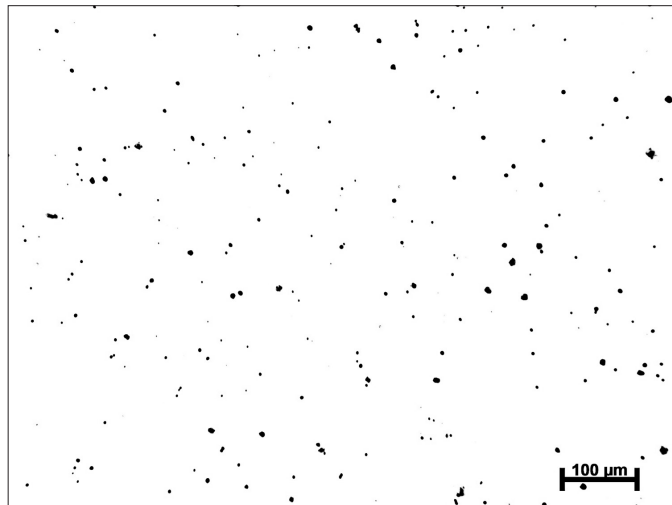


Fig. 1. The non-etched microstructure of Ti6Al4V

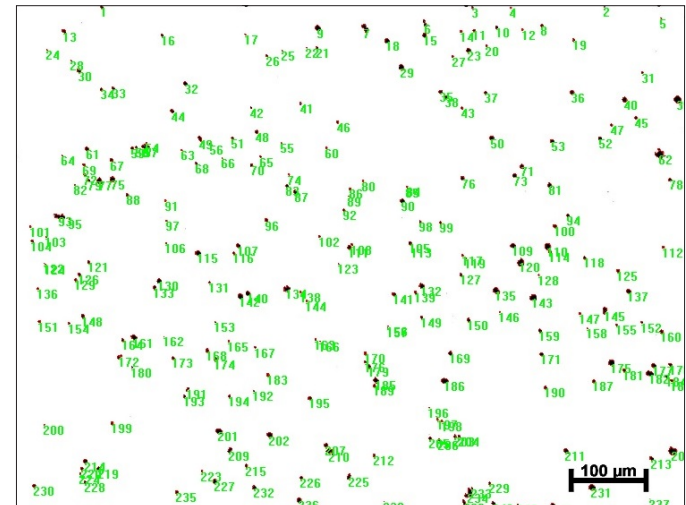


Fig. 2. Software image of Ti6Al4V specimens prepared by AM technology

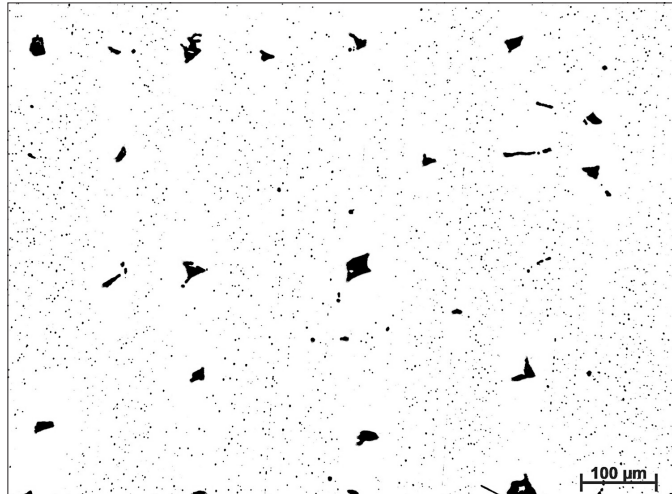


Fig. 3. The non-etched microstructure of CoCrW

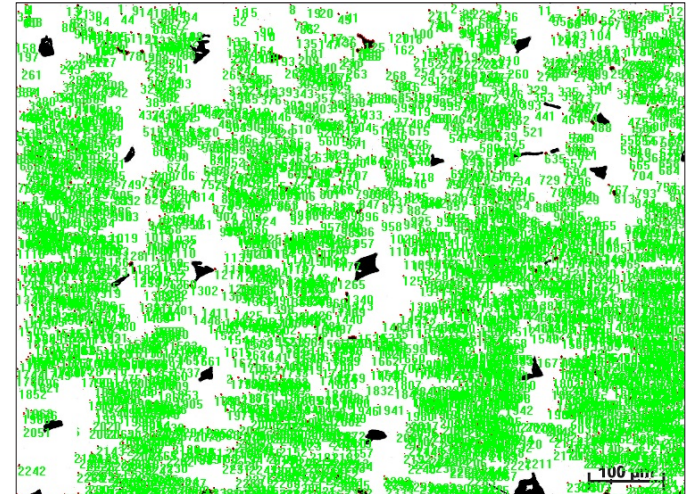


Fig. 4. Software image of CoCrW specimens prepared by AM technology

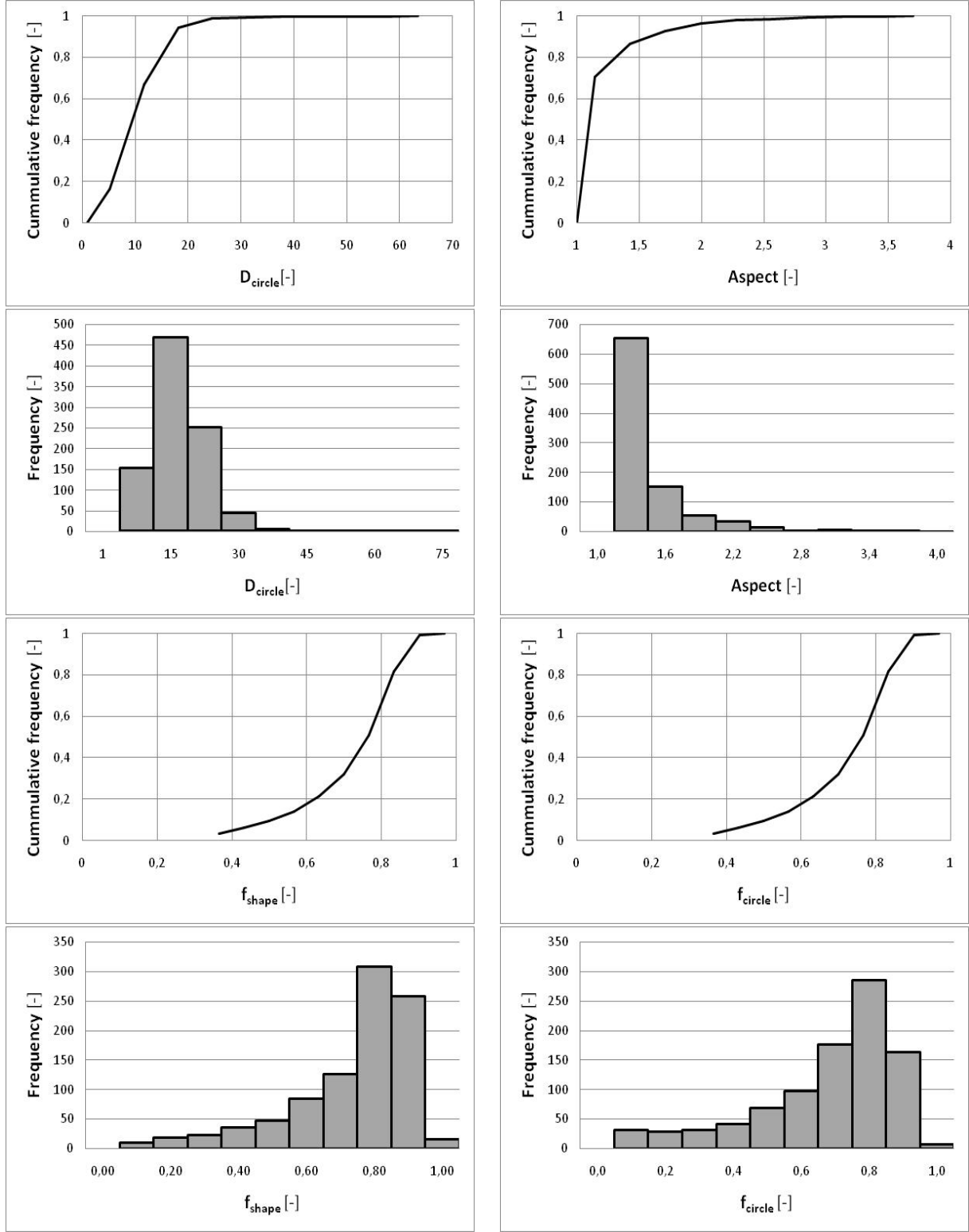


Fig. 5. The distribution histograms and the cumulative frequency of  $D_{circle}$ , Aspect,  $f_{shape}$ , and  $f_{circle}$  in Ti6Al4V

a compressive study to make a comparison between alloy structures on the vital combination of manufacture, microstructures and resulting properties as well as the effects of defects. Porosity affects mechanical properties of AM parts through geometry and distribution of pores. It is well-known that roundness of pores is a key geometrical parameter affecting mechanical properties of the PM materials. These observations are more clearly illustrated

by Fig. 7. The results show that the pore morphology shifts towards rounded morphology of investigated Ti6Al4V alloy (left upper corner). This round-like pore shape (arrow linked to the diagram of pore shape) resulted in better reproduction of the production process and in improved mechanical performance. The relatively good agreement between experiment and theory, based on rounded pore geometry, indicates that the mechanical

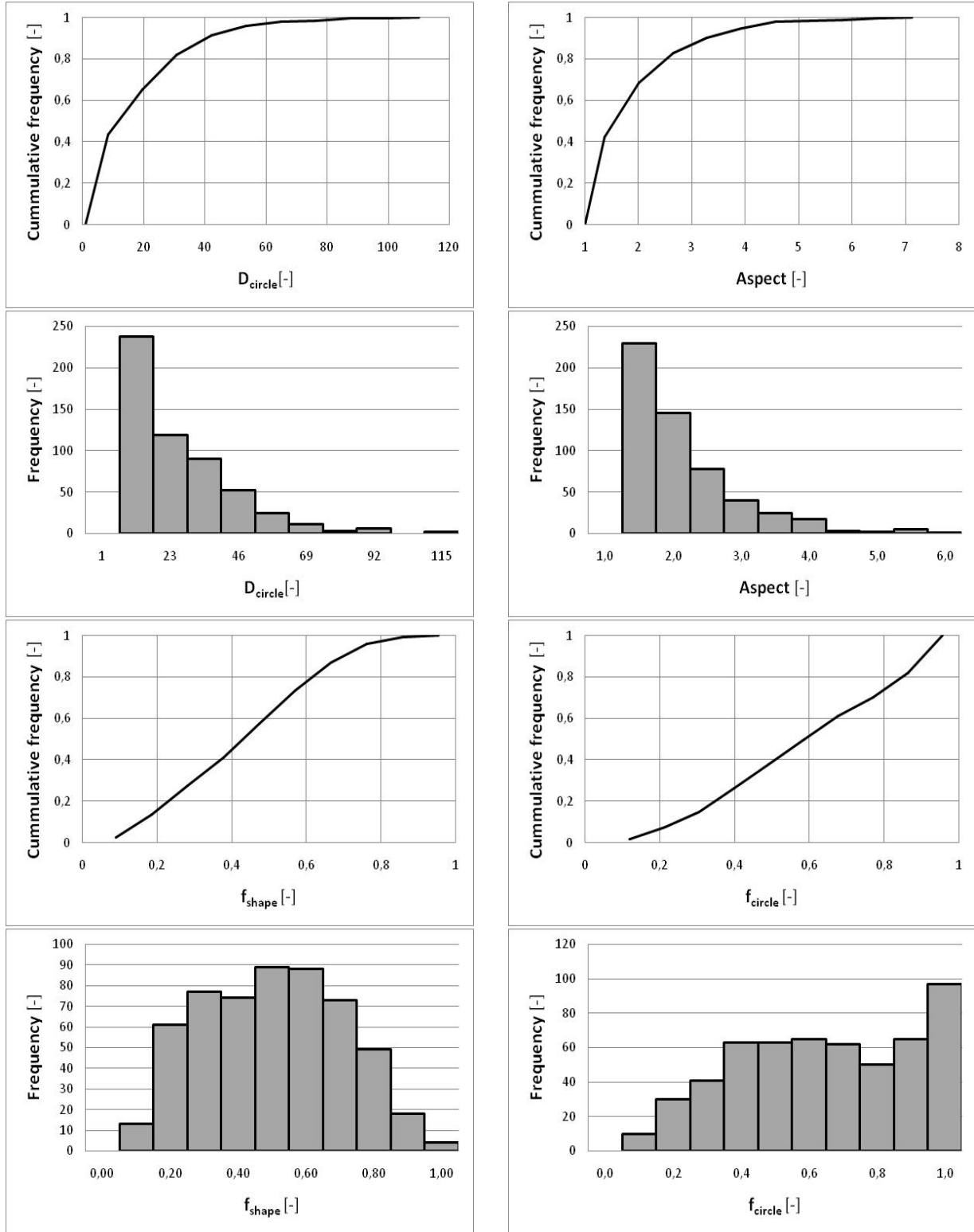


Fig. 6. The distribution histograms and the cumulative frequency of  $D_{circle}$ , Aspect,  $f_{shape}$ , and  $f_{circle}$  in CoCrW

properties of Ti6Al4V alloys do not appear to be significantly influenced by the shape and morphology of the porosity microstructure. On the other hand, CrCoW alloy show a large scatter of pore geometry. More authors [33-35] worked with tungsten alloy underline problem with production process. Zhou et al. [35] found that tungsten high surface tension and viscosity induced a relative slow wetting and spreading speeds, enhancing

the balling phenomenon, which may result in lack of fusion pores. Incomplete fusion holes also known as lack-of-fusion (LOF) defects are mainly due to the lack of energy input during a production process. The formation of the LOF defects is because the metal powders are not fully melted to deposit a new layer on the previous layer with a sufficient overlap. It seems that CoCrW sample was manufactured without contouring side

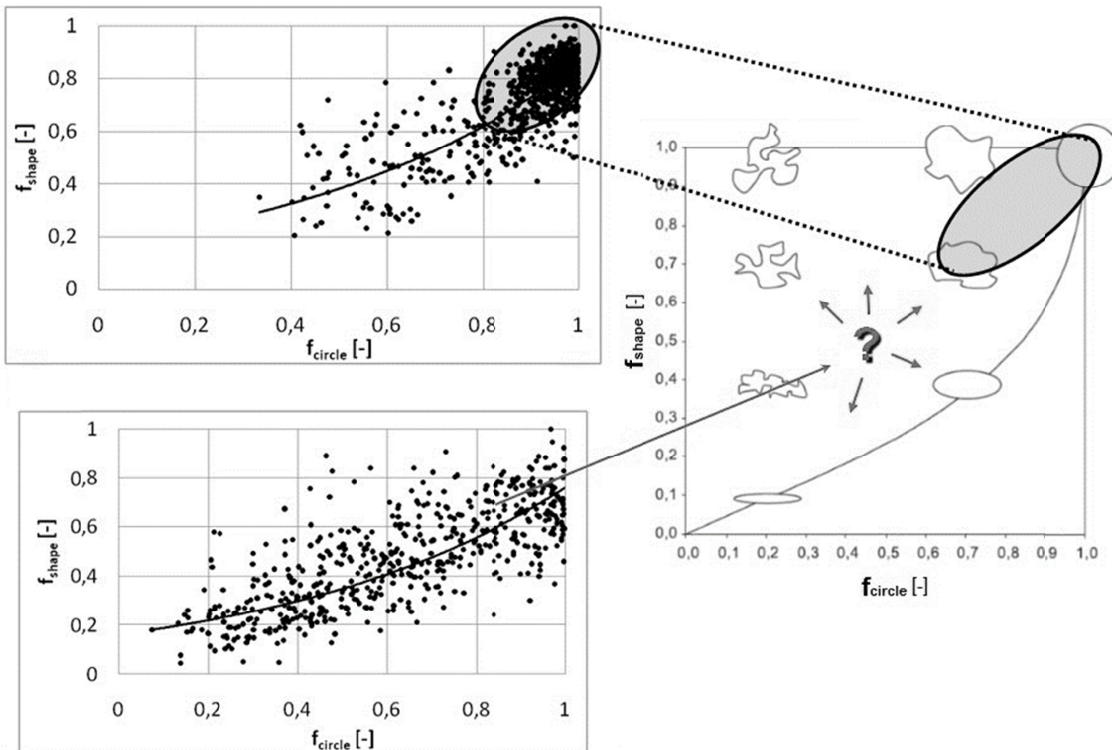


Fig. 7. The results  $f_{circle}$  and  $f_{shape}$  of both alloys

surfaces indicate the presence of balling effect, which confirms the assumption of non-optimal process-parameters [36]. Authors [37] showed, that the pores relating to the LOF have a very spread geometry.

Fig. 7 explains that not only the porosity is an important parameter for the definition of pores or voids in the final part. Also, the ratio of the volume of voids between adjustment particles, as well as the volume of pores, to the volume occupied by the powder, including voids and pores, are important. Moreover, internal factors from processing difficulties can arise while mixing metal powders. AM after each cross-section is scanned, the powder bed is lowered by the one-layer thickness of metal powders, a new layer of metal powder is applied on top, and the process is repeated until the part is completed. The metal powder was mixed with a binder which is then spread over patterned masks and cured layer by layer. Therefore, a complex examination of porosity needs the quantification of morphological and dimensional characteristics, mainly if the proposed based alloys are used in dental applications [23].

#### 4. Conclusions

1. The AM technology is suitable for the preparation of products made from both alloys due to the significant mechanical properties and in terms of porosity evaluation. Mainly it is important note for alloys containing tungsten.
2. Pore size, morphology and distribution of porosity within the building part represent the controlling mechanism of the mechanical response. Also presented results underline that

critical assessment in providing insights into porosity values may be given on pore geometrical factors and distribution.

3. In future fabrication process development, more work focused on the porosity should be considered due to still vast information in comparison with exist information for wrought or cast material.

#### Acknowledgements

Authors are grateful for the support of experimental works by project VEGA 1/0732/16.

#### REFERENCES

- [1] F. Calignano, D. Manfredi, E.P. Ambrosio, S. Biamino, M. Lombardi, E. Atzeni, A. Salmi, P. Minetola, L. Iuliano, P. Fino, Proceedings of the IEEE **105**, 593-612 (2017). DOI: <https://doi.org/10.1109/JPROC.2016.2625098>
- [2] G. Marchese, X.G. Colera, F. Calignano, M. Lorusso, S. Biamino, P. Minetola, D. Manfredi, Adv. Eng. Mater. **19**, 1600635 (2017). DOI: <https://doi.org/10.1002/adem.201600635>
- [3] D. Manfredi, F. Calignano, M. Krishnan, R. Canali, E.P. Ambrosio, E. Atzeni, Materials **6** (3), 856-869 (2013). DOI: <https://doi.org/10.3390/ma6030856>
- [4] L. Yuan, S. Ding, C. Wen, Bioact. Mater. **4**, 56-70 (2018). DOI: <https://doi.org/10.1016/j.bioactmat.2018.12.003>
- [5] C. Zitelli, P. Folgarait, A. Di Schino, Metals **9** (7), 731 (2019), DOI: <https://doi.org/10.3390/met9070731>

- [6] M. Zavala-Arredondo, T. London, M. Allen, T. Maccio, S. Ward, D. Griffiths, A. Allison, P. Goodwin, C. Hauser, Mater. Des. **182**, 108018 (2019).  
DOI: <https://doi.org/10.1016/j.matdes.2019.108018>
- [7] D. Manfredi, R. Bidulsky, Acta Metall. Slovaca **23** (3), 276-282 (2017). DOI: <https://doi.org/10.12776/ams.v23i3.988>
- [8] K.A. Nazari, T. Hilditch, M.S. Dargusch, A. Nouri, J. Mech. Behav. Biomed. Mater. **63**, 157 (2016).  
DOI: <https://doi.org/10.1016/j.jmbbm.2016.06.016>
- [9] L.D. Bobbio, S. Qin, A. Dunbar, P. Michaleris, A.M. Beese, Addit. Manuf. **14**, 60-68 (2017).  
DOI: <https://doi.org/10.1016/j.addma.2017.01.002>
- [10] J.A. Slotwinski, E.J. Garboczi, K.M. Hebenstreit, J. Res. Natl. Inst. Stand. Technol. **119**, 494-528 (2014).  
DOI: <https://doi.org/10.6028/jres.119.019>
- [11] J. Bidulska, R. Bidulsky, M.A. Grande, T. Kvackaj, Materials **12** (22), 3724 (2019). DOI: <https://doi.org/10.3390/ma12223724>
- [12] R. Bidulsky, J. Bidulska, F.S. Gobber, T. Kvackaj, P. Petrousek, M. Actis-Grande, K.-P. Weiss, D. Manfredi, Materials **13** (15), 3328 (2020). DOI: <https://doi.org/10.3390/ma13153328>
- [13] J. Bidulska, T. Kvackaj, I. Pokorný, R. Bidulský, M. Actis Grande, Arch. Metall. Mater. **58** (2), 371-375 (2013).  
DOI: <https://doi.org/10.2478/amm-2013-0002>
- [14] Wohlers Associates. 2012. Additive Manufacturing: Status and Opportunities, Wohlers Associates, Inc.
- [15] R. Bidulsky, J. Bidulska, P. Petroušek, A. Fedoriková, E. Dudrová, M. Actis Grande: Acta Phys. Pol. A **131** (5), 1367-1370 (2017).  
DOI: <https://doi.org/10.12693/APhysPolA.131.1367>
- [16] J. Bidulska, T. Kvackaj, R. Bidulský, M. Actis Grande, Acta Phys. Pol. A **122**, 553-556 (2012).
- [17] E. Poskovic, F. Franchini, M. Actis Grande, L. Ferraris, R. Bidulsky, Acta Metall. Slovaca **23** (4), 356-362 (2017).  
DOI: <https://doi.org/10.12776/ams.v23i4.1032>
- [18] M. Besterici, K. Sulleiova, Acta Metall. Slovaca **25** (1), 65-72 (2019). DOI: <https://doi.org/10.12776/ams.v25i1.1233>
- [19] A. Aversa, M. Lorusso, G. Cattano, D. Manfredi, F. Calignano, E.P. Ambrosio, S. Biamino, P. Fino, M. Lombardi, M. Pavese, J. Alloy. Compd. **695**, 1470-1478 (2017).  
DOI: <https://doi.org/10.1016/j.jallcom.2016.10.285>
- [20] V. Rajčúková, A. Balogová, T. Tóth, R. Hudák, J. Živčák, G. Ižaríková, A. Somoš, M. Kovačevič, Lekar a technika **48** (1), 22-28 (2018).
- [21] J. Bidulská, T. Kvackaj, R. Bidulský, M. Actis Grande, L. Li-tyńska-Dobrzyńska, J. Dutkiewicz, Chem. Listy **105** (16), s471-s473 (2011).
- [22] J. Bidulská, R. Bidulský, M. Actis Grande, T. Kvackaj, Materials **12**, 3724 (2019). DOI: <https://doi.org/10.3390/ma12223724>
- [23] J. Bidulská, R. Bidulský, P. Petroušek, A. Fedoriková, I. Katreničová, I. Pokorný, Acta Phys. Pol. A **131** (5), 1384-1386 (2017). DOI: <https://doi.org/10.12693/APhysPolA.131.1384>
- [24] P. Heinl, L. Müller, C. Körner, R.F. Singer, F.A. Müller, Acta Biomat. **4** (5), 1536-1544 (2008).  
DOI: <https://doi.org/10.1016/j.actbio.2008.03.013>
- [25] J. Alcristo, A. Enriquez, H. Garcia, S. Hinkson, T. Steelman, E. Silverman, P. Valdovino, H. Gigerenzer, J. Foyos, J. Ogren, J. Dorey, K. Karg, T. McDonald, O.S. Es-Said, J. Mater. Eng. Perform. **20**, 203-212 (2011).
- [26] B. Vrancken, L. Thijs, J.-P. Kruth, J. Van Humbeeck, J. Alloys Compd. **541**, 177-185 (2012).
- [27] S. Liu, Y.C. Shin, Mater. Des. **164**, 107552 (2019).  
DOI: <https://doi.org/10.1016/j.matdes.2018.107552>
- [28] B. Ren, C. Chen, M. Zhang, Opt. Eng. **57** (4), 041409 (2018).  
DOI: <https://doi.org/10.1117/1.OE.57.4.041409>
- [29] Y. Lu, Y. Gan, J. Lin, S. Guo, S. Wu, J. Lin, Rapid Prototyp. J. **23** (1), 28-33 (2017).  
DOI: <https://doi.org/10.1108/RPJ-07-2015-0085>
- [30] Y. Lu et al., J. Mech. Behav. Biomed. Mater. **81**, 130-141 (2018).  
DOI: <https://doi.org/10.1016/j.jmbbm.2018.02.026>
- [31] B. Zhang, Y. Li, Q. Bai, Chin. J. Mech. Eng. **30**, 515-527 (2017).  
DOI: <https://doi.org/10.1007/s10033-017-0121-5>
- [32] T. Vilaro, C. Colin, J.D. Bartout, Metall. Mater. Trans. A **42**, 3190-3199 (2011).
- [33] G. Marinelli, F. Martin, S. Ganguly, S. Williams, Int. J. Refract. Met. Hard Mater. **82**, 329-335 (2019).
- [34] B. Nie, L. Yang, H. Huang, S. Bai, P. Wan, J. Liu, Appl. Phys. A **119**, 1075-1080 (2015).  
DOI: <https://doi.org/10.1007/s00339-015-9070-y>
- [35] X. Zhou, X. Liu, D. Zhang, Z. Shen, W. Liu, J. Mater. Process. Technol. **222**, 33-42 (2015).  
DOI: <https://doi.org/10.1016/j.jmatprotec.2015.02.032>
- [36] I. Yadroitsev, P. Krakhmalev, I. Yadroitsava, Addit. Manuf. **7**, 45-56 (2015). DOI: <https://doi.org/10.1016/J.ADDMA.2014.12.007>
- [37] G. Kasperovich, J. Haubrich, J. Gussone, G. Requena, Mater. Des. **105**, 160-170 (2016).